Available online at www.sciencedirect.com
ScienceDirect
International Journal of Hydrogen Energy 32 (2007) 2791–2802
International Journal of HYDROGEN ENERGY
www.elsevier.com/locate/ijhydene

Production of hydrogen from solar zinc in steam atmosphere

Irina Vishnevetsky*, Michael Epstein

Solar Research Facilities Unit, Weizmann Institute of Science, P.O. Box 26, Rehovot 76100, Israel

Received 4 September 2006; received in revised form 21 March 2007; accepted 1 April 2007
Available online 21 May 2007

Abstract

Production of hydrogen via hydrolysis of zinc with steam is an essential step in the Zn/Z nO thermochemical cycle for splitting of water. Recent studies on reducing ZnO to Zn metal with the aid of concentrated solar energy stimulated the interest in the hydrolysis of the zinc for hydrogen production. One of these studies was focusing on solar carbothermal reduction of ZnO to produce zinc powder (EC/FP5-SOLZINC project). The current paper deals with the hydrolysis process of this material which will be referred to, hereafter, as SOLZINC. Test results obtained during the hydrolysis of SOLZINC powder in batch experiments at atmospheric pressure demonstrate possibilities of fast and high conversion of SOLZINC powder with steam to ZnO powder and hydrogen without intermediate melting or evaporation of zinc and indicate that the reaction occurs in two different rates, depending on the preheating temperature. A slow reaction starts at about 250 °C and the hydrogen output increases with reactor temperature. The fast stage starts as the reactor temperature approaches 400 °C. Above this temperature, the reaction develops vigorously due to fast increase of the reaction rate with temperature resulting in releasing additional exothermic heat by the reacted powder. Increasing the preheating temperature (when the steam flow starts) from 200 to 550 °C can improve the SOLZINC conversion during the fast stage from 24% to 81% and increase the hydrogen yield. When the fast stage decays, slow reaction can be continued on for a long time until the hydrogen production is fully achieved.

Keywords: Solar zinc; SOLZINC; Hydrolysis; Hydrogen production; Solar thermochemical cycle; Conversion

1. Introduction

Solar thermochemical cycles for splitting of water, based on hydrolysis of the metal (see Table 1) followed by endothermic reduction of the oxide with the aid of solar energy, could be a promising approach for large-scale production of renewable hydrogen. Thermodynamic analysis of several cycles using different metals, including zinc, was published in the literature already in the seventies and eighties [1]. A review paper [2] discusses possible technical concepts of two-step cycles, suggesting that zinc produced in solar reactors can be considerate as a promising candidate. The common step in these cycles is the hydrolysis of the zinc to produce hydrogen, followed by the second step, e.g. the solar reduction of zinc oxide. Zinc oxide can be decomposed or reduced to zinc in several ways including thermal dissociation of zinc oxide [2,3] and carboreduction with different kinds of solid carbon or natural gas [2,4]. Each of these ways has its own advantages and disadvantages. Despite the absence of CO_2 in the gas product, the main difficulties of the first approach is high temperature (1700–1800 °C) that needs high solar concentration of about 4500 suns, and high temperature construction materials for the reactor. Zinc oxide thermolysis process was demonstrated on lab-scale of 10 kW in a solar reactor heated in a solar furnace [5]. The main challenges of this direct thermolysis approach remain the long-term stability of the reactor materials and the Zn/O_2 products separation resulting in low conversion (about 40%) [5]. In the carbothermal reduction approach, CO_2 gas is present in the product, but the process operating temperature is much lower (1100–1300 °C), and the back reaction can be suppressed down significantly. A remarkable progress was achieved recently with this concept using wood charcoal as a reducing agent of the zinc oxide with the aid of solar energy [4] (in the framework of the EC/FP5 SOLZINC project). A 300 kW pilot scale experiment successfully demonstrated 85–90% conversion at 1100–1200 °C working temperature. It was advantageous to form the zinc as a powder in the solar process due to easier

* Corresponding author. Tel.: +972 8 9342284; fax: +972 8 9344117.
E-mail address: irina.vishnevetsky@weizmann.ac.il (I. Vishnevetsky).

0360-3199/$ - see front matter © 2007 International Association for Hydrogen Energy. Published by Elsevier Ltd. All rights reserved.
doi:10.1016/j.ijhydene.2007.04.004

Nomenclature

C	concentration
C^0_{Zn}	zinc concentration in loaded Zn powder
C_{H_2}	hydrogen concentration in output gases
C_{Zn}	real zinc concentration in ZnO powder after test
C^{ideal}_{Zn}	theoretical zinc concentration in ZnO powder that would be obtained without Zn losses
C^{max}_{Zn}	maximal possible zinc concentration in ZnO powder
C^{max}_{Zn}	minimal possible zinc concentration in ZnO powder
$Conv._{H_2}$	zinc conversion calculated from hydrogen yield
F	volumetric flow rate
F_{in}	input gas flow rate
F_{out}	output gas flow rate
F_{H_2}	hydrogen flow rate
F_{N_2}	nitrogen flow rate
F^{gas}_{Zn}	zinc gas flow rate
ΔF	flow rate difference
H	enthalpy
ΔH	enthalpy difference between products and reactants
L, l	losses
L_{Zn}	total zinc losses
l^{solid}_{Zn}	solid zinc losses
$l^{gas(n/r)}_{Zn}$	gas zinc losses non-reacted
$l^{gas(r)}_{Zn}$	gas zinc losses reacted
l^{gas}_{Zn}	gas zinc losses total
M, m	mass
$\dot{M}$	mass flow rate
$\dot{M}_{H_2O}$	water mass flow rate
Δm	mass difference
M_0	mass of loaded zinc powder
M^0_{Zn}	mass of Zn in loaded zinc powder
M_1	real mass of ZnO powder after test
M^{ideal}_1	theoretical mass of ZnO powder that would be obtained without Zn losses
$m^{empty}_{(s-h)0}$ and $m^{empty}_{(s-h)1}$	mass of empty sample holder before and after test
$m^{full}_{(s-h)0}$ and $m^{full}_{(s-h)1}$	mass of full sample holder before and after test
P	total pressure
P_0	total pressure in reactor before steam flow starts
P_{max}	maximal total pressure
P_{H_2O}	steam partial pressure
$P^0_{H_2O}$	basic steam partial pressure (without reaction)
$P^{ideal}_{H_2O}$	steam partial pressure would be without Zn losses
$Prod._{H_2}$	Zn powder productivity (amount of hydrogen per g of loaded powder)
T	absolute temperature
t	celsius temperature
$t_{r\text{-}zone}$	temperature in reaction zone
$t_{steam\ flow\ start}$	temperature in reaction zone when the steam flow starts
$t_{Pyrex\ beads}$	temperature in the upper part of Pyrex beads
V	volume
V_{H_2}	hydrogen yield
μ	molecular weight
μ_{Zn}	zinc molecular weight
μ_{ZnO}	zinc oxide molecular weight
μ_O	oxygen molecular weight
μ_{H_2O}	water molecular weight
τ	time

quenching of the product gases and the handling of the stored solid zinc.

Solar zinc powder produced in this pilot scale tests was available in amount of over 500 kg [4] and was used as the base material for the current hydrolysis experiments at moderate reactor temperature (below 600 °C) and atmospheric pressure in oxygen deficient atmosphere.

The zinc hydrolysis exothermic process proceeds according to

$$Zn + H_2O = ZnO + H_2, \quad \Delta H_{500\,^\circ C} = -110.3\,kJ. \tag{1}$$

Although the hydrogen productivity of zinc hydrolysis is lower compared with other metal hydrolysis reactions because of its high molecular weight and relatively low valence (see Table 1), the advantage of zinc hydrolysis is its simple chemistry. The single problem is zinc evaporation and its possible interaction with the container materials which can cause zinc losses as the temperature is increased.

Very little information is available in the literature about the hydrolysis of zinc powder. Thermogravimetric analyses of hydrolysis of commercial zinc powder (by Merck, purity 99%, 10 μm particle size) at temperature 350–500 °C and solar zinc powder obtained by the thermolysis of ZnO in a solar furnace (purity 98%, 9 μm particle size) are presented in [6]. The hydrolysis reaction rate of the solar zinc was significantly higher than the commercial zinc but stayed very slow (less than 0.6% mass gain/min). The solid product in these reactions was not a powder but rather black hard sintered material with zinc content of about 50% for the commercial zinc and grey porous voluminous material with a zinc content of less than 10% for the solar zinc.

Other detailed studies on the kinetics of hydrogen production via the hydrolysis of liquid zinc by means of bubbling water

Table 1
Theoretical hydrogen productivity of different hydrolysis reactions

Reaction	STP				
	Mole H_2 per g-reactants	Mole H_2 per g-metal	L H_2 per g-metal	g-Metal oxide per mole H_2	$\Delta H_{773\,K}$ kJ/g-Me
$2B + 3H_2O \rightarrow 3H_2 + B_2O_3$	0.0396	0.139	3.00	23.21	−23.4
$2Al + 3H_2O \rightarrow 3H_2 + Al_2O_3$	0.0278	0.056	1.25	33.99	−17.7
$Mg + H_2O \rightarrow H_2 + MgO$	0.0236	0.041	0.92	40.31	−14.6
$Fe + H_2O \rightarrow H_2 + FeO$	0.0135	0.018	0.40	71.85	−0.66
$Zn + H_2O \rightarrow H_2 + ZnO$	0.0120	0.015	0.34	81.41	−1.69

vapor through a bath at 450–520 °C can be found in the literature [7], or direct hydrolysis of zinc vapor, generated at 990 °C from liquid zinc, with steam [8]. In both cases, the liquid zinc was prepared by melting of solid commercial granules.

The aim of the present work was to investigate the hydrolysis process of zinc powder as a function of carefully controlled parameters such as temperature, water flow or steam partial pressure, steam to metal ratio, metal structure, its dispersion and purity, with a purpose to minimize zinc losses and maximize the conversion of the metal powder to the metal oxide powder inside the sample holder. A special test apparatus was developed for this study. Results obtained during a batch hydrolysis testing of 10 g SOLZINC powder, compared with commercial zinc powder by Sigma-Aldrich at reactor temperature below 600–620 °C, normal total pressure and water mass flow rate of 0.55 g/min are presented.

2. Experimental

2.1. Experimental setup; instrumentation and accuracy

A scheme of the test setup is presented in Fig. 1. This setup with some modifications has been used also for boron hydrolysis study [9]. The main elements of the apparatus are two vertical cylindrical ovens (2 and 4 in Fig. 1), made of ceramic fibers containing electrical heating elements (made by WATLOW). One oven with a power rating of 1.7 kW heats the spiral boiler (1), made of 1/8 in stainless steel tube, and the second, whose power rating is 2.2 kW, is wrapped around a stainless steel reactor tube with 1 in outer diameter (6).

The water is fed into the boiler (1) by a piston micro-metering pump (14) (made by Autoclave Engineering, series MMP1). Pump flow rate can be regulated with an accuracy of 3% in the range of 0.01–10 ml/min. Superheated steam at temperature of above 500 °C can be obtained at the boiler exit. During the preparatory stage of the test, the boiler is cleaned by blowing steam through it, and the reactor is washed out with the carrier gas (N_2). When the pre-determined test temperature of the reactor is reached, the steam is mixed with the carrier gas, and the gas mixture is fed into the reactor tube, where it is heated further, up to 650 °C, while flowing through a bed of Pyrex beads located in the lower part of the reactor tube (6). A powder sample holder (5) with holes in its bottom is located in the reactor, just above the Pyrex beads. Its outer diameter is equal to the inner diameter of the reactor tube. Sample holder is lined by zirconia felt and can hold up to 30 cm^3 of solid reactant.

The option of continuous feeding of powder is provided in the upper part of reactor (not shown in Fig. 1). In this case, the carrier gas with the powder could be fed to the upper part of reactor from a vibrating micro-metering feeder.

Control of the electrical energy input is facilitated by two thermocouples located, respectively, at the upper part of the boiler tube near its exit (TC2) and in the upper part of the beads layer, near the reaction zone in the central part of the reactor (TC5). The temperature in the reaction zone is measured by thermocouple TC4, placed inside sample holder. Thermocouples TC1 and TC3 are used to control the temperatures of the outer tube walls of the boiler and reactor. All the thermocouples are K-type (Chromel–Alumel with Inconel 600 sheath), 1.5 mm in diameter and 1 m long. Temperature measurement accuracy was within 1%.

Following the reactor, the gas–steam mixture passes through water cooling steam condenser (8), and dry ice trap (9) to decrease humidity in the outer measuring part of system. Two filters are also installed upstream the measurement devices for their full protection.

The apparatus inter-connecting pipelines contain four high temperature regulating needle valves (NV) and are heated by OMEGA trace heaters (3,7). Trace heaters are controlled at a temperature of 150–200 °C to prevent steam condensation in the pipes.

Inlet and exit gas flow rates are measured by Tylan General Mass Flow meters FM-360 with accuracy of 1% of FS. Nitrogen is used as a carrier gas. Its flow is measured by flow meter (13) with a span of 500 cm^3/min placed after the supply cylinder. Flow-out of H_2 and N_2 mixture is measured by flow-meter (12) (span 1500 cm^3/min) or (11) (span 300 cm^3/min) depending on the reaction conditions and hydrogen output. Simultaneous on-line analysis of hydrogen content is carried out with a multi-auto range hydrogen analyzer (Calomat 6, by Siemens) calibrated with H_2–N_2 mixture. The error in determining the gas composition, including the calibration mixture and response time of analyzer, was estimated as 5%.

The reaction pressure can be regulated by the back-pressure valve, NV4, installed at the reactor exit. Pressure control is carried out by three STS pressure transmitters with accuracy of 2–3%, installed at the entrance to the reactor (PT1), before the back pressure valve (PT2) and at the exit of the dry ice trap (PT3).

Recording of experimental data was done in 10 s intervals using Data Acquisition Modules ADAM-4018 and ADAM-4017 (by Advantech).

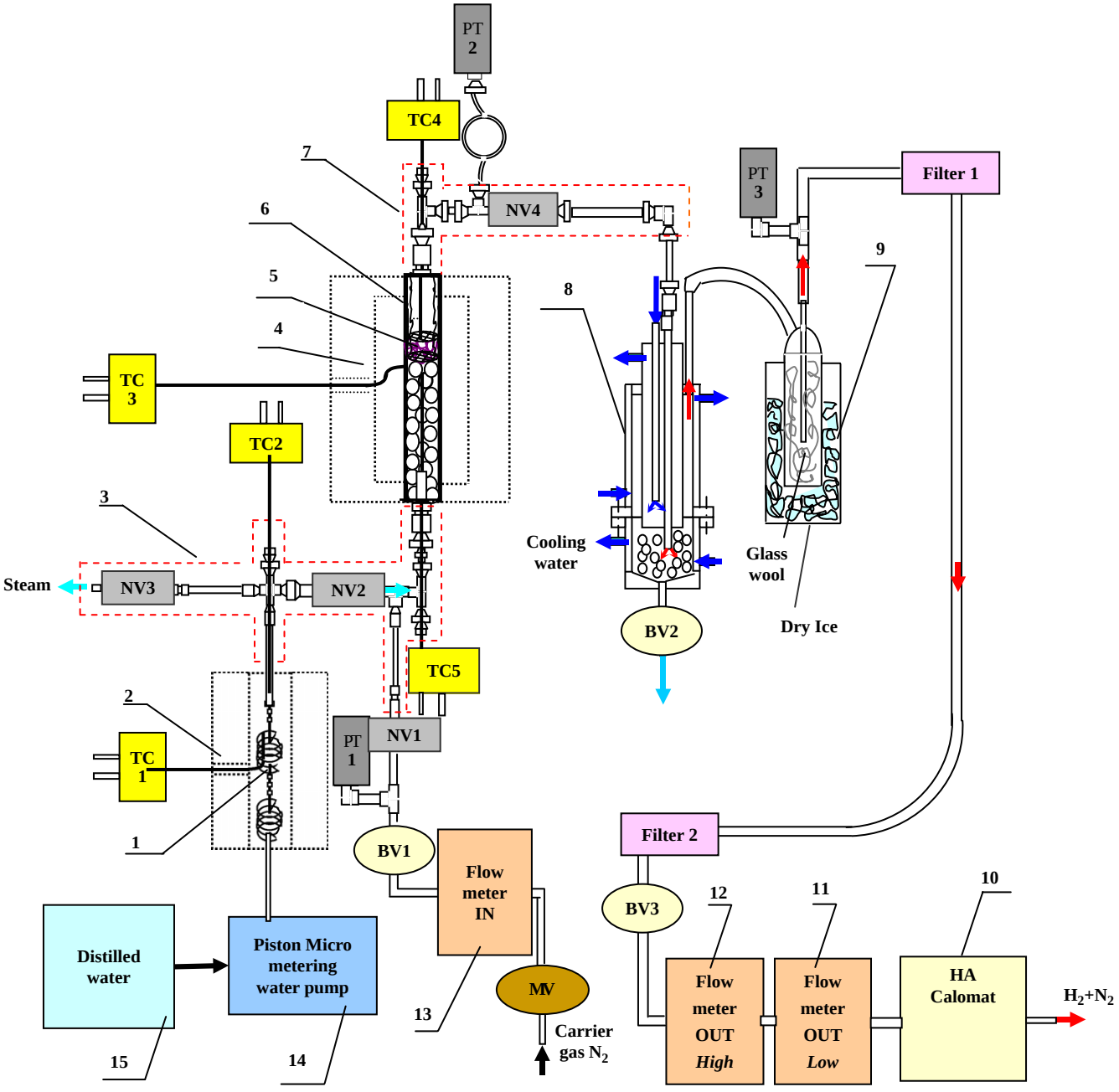

Fig. 1. Schematic layout of the test setup: (1) boiler tube; (2) boiler oven; (3, 7) trace heaters; (4) reactor oven; (5) sample holder; (6) reactor tube; (8) condenser; (9) dry ice trap; (10) hydrogen analyzer; (11–13) flow meters; (14) piston micro-metering water pump; (15) container with distilled water; TC-thermocouple; PT-pressure transmitter; NV-needle valve; BV-ball valve; MV-metering valve.

The sample holder is filled with grey Zn powder before test and contains white-gray mixture of ZnO and Zn powder after the test, as shown in Fig. 2. Examination of the inner surface of the sample holder after test reveals a thin layer resulting from zinc interaction with the stainless steel. Therefore, the weight of the empty sample holder is also slightly increased, depending on the preheating temperature. In conclusion, increasing the temperature causes zinc losses of three kinds: non-reacted solid (alloying with the sample holder walls), non-reacted gas (pre-reaction evaporation of zinc before the steam flow starts) and reacted gas (zinc evaporation occurring during the process of hydrolysis). It should be noted that Zn or ZnO cladding on the internal surface of the pipes downstream the reactor were, practically, not observed.

2.2. The main experimental parameters

The main input and output parameters (measured and calculated) and their units are presented in Table 2 (See Nomenclature).

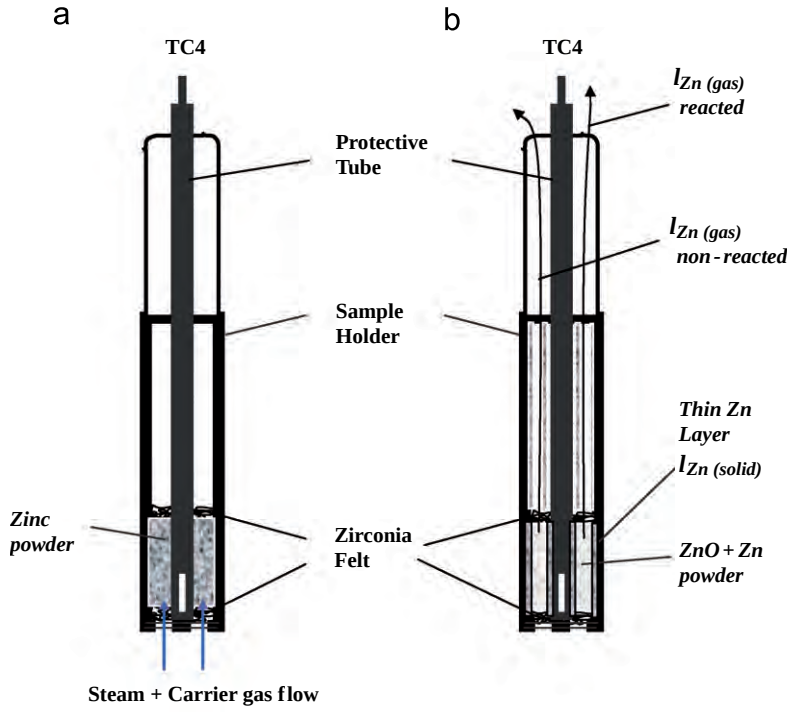

Fig. 2. Sample holder (a) before and (b) after test.

Table 2
The main input and output parameters

Input parameters		Output parameters		
Measured	Calculated	Measured	Calculated	
$t_{\text{steam flow start}}$ (°C)	M_0 (g)	$t_{\text{r-zone}}$ (°C)	M_1 (g)	l_{Zn}^{solid} (g) (%)
$F_{in} = F_{N_2}$ (STP cm^3/min)	M_{Zn}^0 (g)	$t_{\text{Pyrex beads}}$ (°C)	M_1^{ideal} (g)	$l_{Zn}^{gas(n/r)}$ (g) (%)
$\dot{M}_{H_2O}$ (g/min)	$P_{H_2O}^0$ (bar)	$F_{out} = F_{N_2+H_2}$ (STP cm^3/min)	F_{H_2} (STP cm^3/min)	$l_{Zn}^{gas(r)}$ (g) (%)
P_0 (bar)		P (bar)	V_{H_2} (STP cm^3)	l_{Zn}^{gas} (g) (%)
$m_{(s-h)0}^{empty}$ (g)		$m_{(s-h)1}^{empty}$ (g)	Conv_{H_2}	L_{Zn} (g) (%)
$m_{(s-h)0}^{full}$ (g)		$m_{(s-h)1}^{full}$ (g)	C_{Zn}^{ideal}	P_{H_2O} (bar)
C_{Zn}^0		C_{Zn}	C_{Zn}^{max}	$P_{H_2O}^{ideal}$ (bar)
		C_{H_2}	C_{Zn}^{min}	Prod._{H_2} (cm^3/g)

2.3. Calculation of the main parameters

The hydrogen output flow rate, its yield, temperature variations in the exothermic reaction zone and the weight of the powder in sample holder left after the reaction can be used for estimating the reaction rate, zinc conversion and its losses as a function of important parameters such as temperature in the reaction zone when the steam flow starts, water mass flow rate (or steam partial pressure) and steam to Zn ratio.

The initial mass of the SOLZINC powder, M_0, was calculated as the difference between the full and the empty sample holder mass before the test, whereas the mass of the remaining powder, M_1 (a mixture of zinc oxide and unreacted zinc), was calculated as the difference between the mass of the full and empty sample holder after the test (balance SA 80, max 80 g with 100 μg resolution, by SCINTECH was used for all weighing measurements):

$$M_0 = \Delta m_{(s-h)0}^{\text{full-empty}}, \tag{2}$$

$$M_1 = \Delta m_{(s-h)1}^{\text{full-empty}}. \tag{3}$$

The content of the initial pure zinc in the SOLZINC powder is calculated as

$$M_{Zn}^0 = C_{Zn}^0 M_0. \tag{4}$$

The hydrogen flow rate was calculated in two ways:

$$F_{H_2} = F_{out} - F_{in} = \Delta F, \tag{5}$$

$$F_{H_2} = F_{out} * C_{H_2}, \tag{6}$$

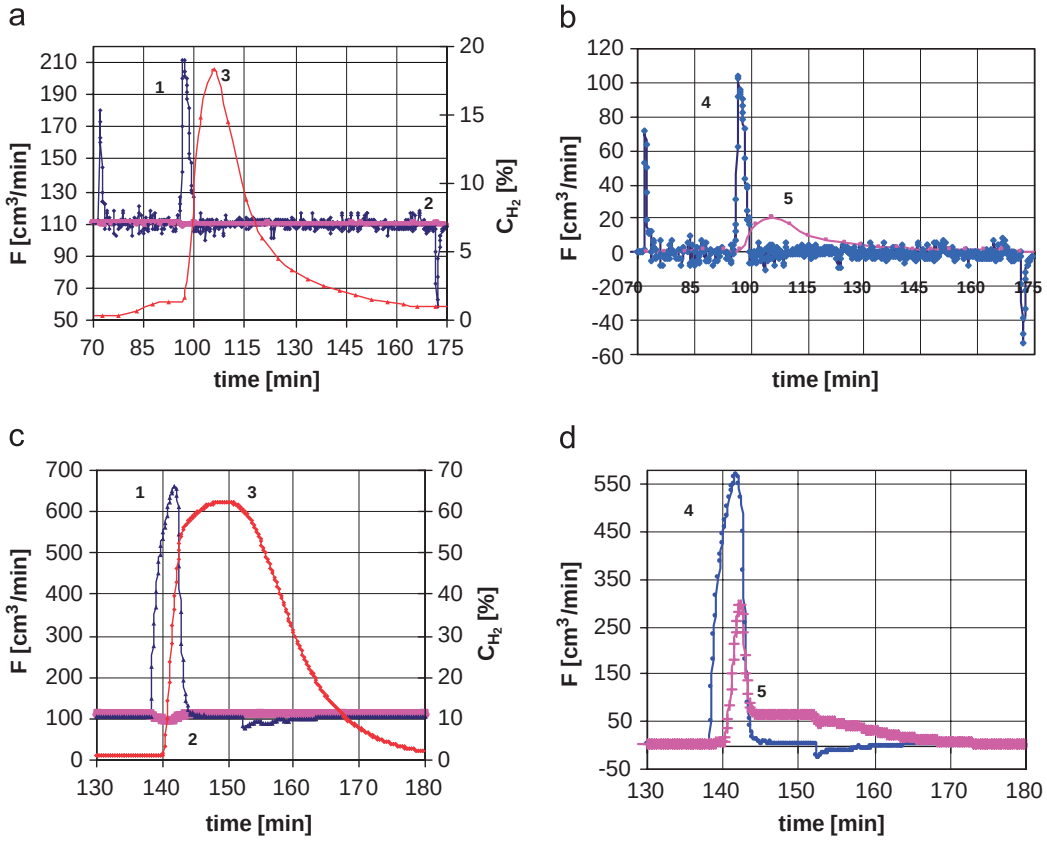

Fig. 3. Flow parameters: (1) F_{out}; (2) F_{in}; (3) C_{H_2}; (4) ΔF; (5) F_{H_2} (a, b: steam flow starts at 250 °C; c, d: steam flow starts at 550 °C), amount of zinc ≈ 9–10 g.

where C_{H_2} is the hydrogen volumetric concentration determined by the analyzer (10 in Fig. 1) and F_{in}, F_{out} (cm^3/min) are the total inlet and outlet flow rates without steam (see Fig. 3).

Each one of these flow measurements has its own advantages and disadvantages. Hydrogen flow rate calculated as ΔF (Eq. (5)) provides an immediate indication about its formation because the hydrogen displaces out an equivalent volume of N_2 from the condenser and traps. (The flow meter conversion factor for H_2–N_2 mixture agrees within 1–1.8% with the N_2 factor, therefore the flow calculations can be done without considering the hydrogen concentration.) When the hydrogen evolution rate is relatively high (50–500 cm^3/min, for example) hydrogen flow can be determined within an error range of 10–3.5%, respectively. Flow out is sensitive not only to hydrogen formation but also to temporary changes in pressure inside the reactor caused, for example, by starting and stopping of the steam flow (see the first and last peaks in curve 1 (Fig. 3a, b)). These interfering steam peaks are corrected by measuring them at the same condition but with the absence of solid reactant. Additional inaccuracy can be caused by Zn evaporation. However, comparing total hydrogen yield calculated by Eq. (7) (see below) versus calculations of $F_{H_2}(\tau)$ from Eqs. (5) and (6) separately shows that this error was less than 2–3%.

If the reaction rate is low and the hydrogen output does not exceed a few cm^3/min, calculation according to Eq. (5) can lead to a large error and can be used only as indicative information. In this case, Eq. (6) allows estimating the low hydrogen flow rate within 5–10% error, but it takes 5–15 min delay to obtain a measurement, depending on the hydrogen yield. Hydrogen peak is smoothed over a larger time period because of the mixing with nitrogen in the condenser and the trap. Eq. (5) is therefore used when the reaction rate is fast, whereas the results of Eq. (6) are closer to the real hydrogen output of the setup. The accumulative volume of H_2 at standard conditions can be calculated by integrating the curve of hydrogen flow over the relevant time period.

$$V_{H_2} = \int_{\tau_1}^{\tau_2} F_{H_2}\, d\tau. \tag{7}$$

Using the data about the real hydrogen yield and the theoretical amount of hydrogen yield per gram of zinc (see Table 1), the zinc conversion can be calculated as

$$\text{Conv.}_{H_2} = \frac{V_{H_2}}{340 C^0_{Zn} M_0} \tag{8}$$

(340 is the theoretical productivity of reaction (1) in STP cm^3 H_2 per g-zinc) whereas the productivity of the loaded powder is defined as

$$\text{Prod.}_{H_2} = \frac{V_{H_2}}{M_0}. \tag{9}$$

The calculations of the theoretical amount of material that could be obtained after the reaction is stopped (assuming no losses

of zinc) and the theoretical Zn concentration in such imaginary final material can be calculated as

$$M_1^{\text{ideal}} = M_0\left(1 + C_{\text{Zn}}^0 \text{Conv.}_{\text{H}_2}\frac{\mu_{\text{O}}}{\mu_{\text{Zn}}}\right), \tag{10}$$

$$C_{\text{Zn}}^{\text{ideal}} = \frac{C_{\text{Zn}}^0 M_0(1-\text{Conv.}_{\text{H}_2})}{M_1^{\text{ideal}}}. \tag{11}$$

The actual weight of powder found in the sample holder after the test is terminated (using Eq. (3)) and the actual non-reacted zinc concentration in this material (measured in parallel by Ultra III Rigaku X-ray powder diffractometer) can be written as

$$M_1 = M_1^{\text{ideal}} - L_{\text{Zn}}, \tag{12}$$

$$C_{\text{Zn}} = \frac{C_{\text{Zn}}^0 M_0(1-\text{Conv.}_{\text{H}_2}) - (l_{\text{Zn}}^{\text{solid}} + l_{\text{Zn}}^{\text{gas}(n/r)})}{M_1}. \tag{13}$$

The total zinc losses are

$$L_{\text{Zn}} = l_{\text{Zn}}^{\text{solid}} + l_{\text{Zn}}^{\text{gas}} = l_{\text{Zn}}^{\text{solid}} + l_{\text{Zn}}^{\text{gas}(n/r)} + l_{\text{Zn}}^{\text{gas}(r)}\ \text{(g)}. \tag{14}$$

The loss of solid zinc is estimated as the difference of the weight of the empty sample holder after and before the test:

$$l_{\text{Zn}}^{\text{solid}} = \Delta m_{(s-h)1-0}^{\text{empty}-\text{empty}}\ \text{(g)}, \tag{15}$$

whereas the gas losses $l_{\text{Zn}}^{\text{gas}(r)}$, $l_{\text{Zn}}^{\text{gas}(n/r)}$ are unknown and can be expressed from the set of Eqs. (12), (13) as

$$l_{\text{Zn}}^{\text{gas}(n/r)} = C_{\text{Zn}}^0 M_0(1-\text{Conv.}_{\text{H}_2}) - C_{\text{Zn}} M_1 - l_{\text{Zn}}^{\text{sol}} \geqslant 0\ \text{(g)}, \tag{16}$$

$$l_{\text{Zn}}^{\text{gas}(r)} = M_0(1-C_{\text{Zn}}^0) - M_1(1-C_{\text{Zn}}) + C_{\text{Zn}}^0 M_0\,\text{Conv}_{\text{H}_2}\frac{\mu_{\text{ZnO}}}{\mu_{\text{Zn}}} \geqslant 0\ \text{(g)} \tag{17}$$

and

$$l_{\text{Zn}}^{\text{gas}} = M_0\left(1 + C_{\text{Zn}}^0\,\text{Conv}_{\text{H}_2}\frac{\mu_{\text{O}}}{\mu_{\text{Zn}}}\right) - (M_1 + l_{\text{Zn}}^{\text{sol}}). \tag{18}$$

To calculate the zinc losses in percents of the initially loaded zinc, the values in grams are estimated from Eqs. (14) to (18) and divided by the mass of the loaded zinc, M_{Zn}^0 (see Eq. (4)).

It is also possible to estimate the range of the actual unreacted zinc concentration in the remaining powder by calculating the low and high limits of C_{Zn} using Eqs. (16) and (17):

$$C_{\text{Zn}} \geqslant \frac{1}{M_1}\left(M_1 - M_0(1-C_{\text{Zn}}^0) - C_{\text{Zn}}^0 M_0\,\text{Conv.}_{\text{H}_2}\frac{\mu_{\text{ZnO}}}{\mu_{\text{Zn}}}\right) = C_{\text{Zn}}^{\min}, \tag{19}$$

$$C_{\text{Zn}} \leqslant \frac{1}{M_1}(C_{\text{Zn}}^0 M_0(1-\text{Conv.}_{\text{H}_2}) - l_{\text{Zn}}^{\text{solid}}) = C_{\text{Zn}}^{\max}. \tag{20}$$

This estimation is very useful to check the reliability of the measured C_{Zn}, especially for low values. The problem lies in the sensitivity of the measured concentration values not only to the experimental error of the X-ray device but also to the database that is used for the treatment of the results, to structure coincidence of sample composites with reference materials.

Generally, the steam partial pressure can be written as

$$P_{\text{H}_2\text{O}} = \frac{P}{1+(a/\dot{M}_{\text{H}_2\text{O}}(\text{g/min}))(F_{\text{N}_2}+F_{\text{H}_2}+F_{\text{Zn}}^{\text{gas}})(\text{cm}^3/\text{min})}. \tag{21}$$

Here

$$a = \frac{\mu_{\text{H}_2\text{O}} P_{\text{norm}}}{8.31 T_{\text{norm}}}10^{-6}(\text{g/cm}^3);$$

$$(P_{\text{norm}} = 10^5(\text{N/m}^2),\ T_{\text{norm}} = 300\,\text{K}).$$

The flow rate of the zinc gas losses, $F_{\text{Zn}}^{\text{gas}}$, is practically impossible to measure. However, the total zinc vapor losses (see below, Fig. 7a) are estimated to be less than 4%. Therefore, the zinc gas flow compared to the nitrogen flow in the experiments ($F_{\text{N}_2} \approx 100\,\text{cm}^3/\text{min}$) is negligible and therefore, practically, $P_{\text{H}_2\text{O}} \approx P_{\text{H}_2\text{O}}^{\text{ideal}}$.

3. Zn powders' main characteristics

SOLZINC powder of typically a few microns size [4] was used for most tests. According to the X-ray, results of samples from different production runs contain 10–15% ZnO. For comparison a commercial Zn powder (by Sigma-Aldrich, Cat.:20998-8) with purity of 98% and $< 10\,\mu\text{m}$ size was used. Structure of both powders can be seen below in Fig. 9.

4. Results and discussion

4.1. Typical variation of main parameters versus time

Typical parameters and results of the first test using SOLZINC powder are shown in Fig. 4. Initially, the reactor is heated at a rate of 5–6 °C/min and when the desirable temperature level of 180–250 °C was reached, the steam was fed into the reactor (the first peak on curve 5 in Fig. 4a is caused by steam flow displacing out nitrogen from the system and is not a result of hydrogen generation; fluctuation in the low part of curve 5 are explained by water feeding pulses caused by the piston pump). Few minutes later, when the temperature in the reaction zone approaches 300 °C, the hydrogen analyzer begins to sense the hydrogen amounting at few percentages, which increases as the temperature rises (not shown in this figure). Output flow also increases slowly (curve 5). As the temperature in the reaction zone approaches 400 °C, a vigorous reaction is developed, and the output flow and temperature in the reaction zone rise strongly (the second peak in curve 5 is caused by the displacement of nitrogen resulting from hydrogen production). This can last for few minutes and then the exit flow and the temperature in the reaction zone begin to decrease, but the reaction does not stop completely. It continues at a lower rate similar to that prior to the vigorous reaction in spite of the higher temperature in the reaction zone.

It should be noted here that thermocouple (TC4) measures the bulk temperature in the sample holder (reaction zone) and not the temperature of the zinc particle itself, where the exothermic reaction happens.

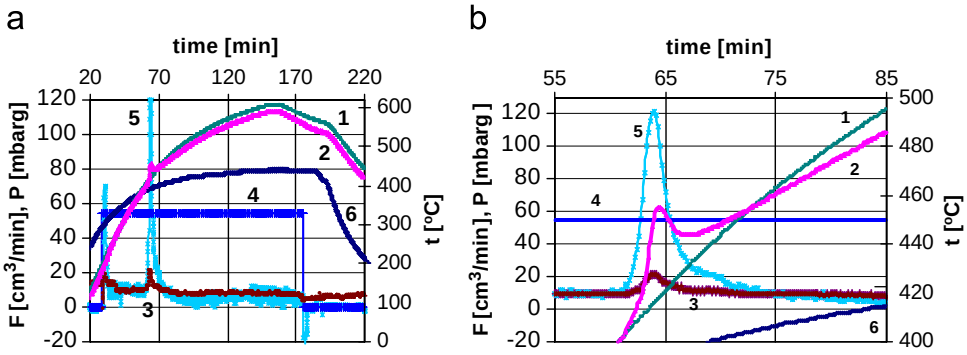

Fig. 4. The main parameters of SOLZINC powder hydrolysis versus time from beginning of heating (8.9 g sample), a: full test; b: hydrogen peak area; (1) temperature in the upper part of Pyrex bead layer (TC5); (2) temperature in reaction zone (TC4); (3) pressure in reactor (PT2); (4) water flow rate ∗ 100 from pump; (5) hydrogen flow rate from Eq. (5); (6) steam temperature at the exit of boiler (TC2).

Table 3
Operating conditions and main characteristics for zinc hydrolysis tests

No.	M_0 (g)	M_1 (g)	l_{Zn}^{solid} (g)	$t_{r\text{-zone}}$ steam flow starts (°C)	$t_{r\text{-zone}}$ fast reaction begins (°C)	$t_{max\ in}$ reaction zone (°C)	P_0 (mbar g)	P_{max} (mbar g)	Prod.$_{H_2}$ in peak (cm^3/g)	Conv.$_{H_2}$ in fast peak (%)	Conv.$_{H_2}$ full (%)	C_{Zn} in powder (after test) (%)
1	***2***	***3***	***4***	***5***	***6***	***7***	***8***	***9***	***10***	***11***	***12***	***13***
1	8.85	9.81	0.05	185	400	454	56	64	69	24.0	67.7	–
2	9.7	10.49	0.15	393	393	553	60	105	119	43.5	51.0	35.5
3	9.95	11.22	0.21	443	443	601	67	122	189	66.2	73.7	16.0
4	9.42	10.89	0.30	510	510	700	67	157	233	80.9	87.8	4.7
5	10.4	12.00	0.67	560	560	742	65	172	232	80.6	88.5	1.3
6[a]	10.33	10.95	0.35	518	518	577	73	132	79	23.6	29	–

[a]Zinc powder from Sigma-Aldrich.

It should be noted also that the developing of the zinc hydrolysis process is similar to that of the boron, studied earlier [9]. In both cases there is a slow stage occurring at lower temperature. Due to low reaction rate, the negligible amount of exothermic heat cannot affect the temperature in the reaction zone. As the temperature is increased and the reaction rate becomes higher, the released heat is increased and the process suddenly becomes very fast. This fast stage decays as the amount of the solid reactant in the sample holder is depleted, the rate of the released heat is decreased and the reaction returns to slow rate. The slow stage is also sensitive to the temperature. The hydrogen production follows the variations in temperature that were initiated during the first and second steps of the slow stage (Fig. 4a).

The fast stage in zinc hydrolysis starts at temperature around 400 °C. However, the zinc fast stage conversion in this case is only 25%. One option to improve the conversion is to start the steam flow at higher temperatures, above 400 °C. Postponing the beginning of the reaction to higher temperature could result in higher particle's temperature and faster reaction rate. In addition, this can avoid the low temperature slow stage, decrease the amount of zinc oxide accumulated in the powder before the fast reaction develops and save some exothermic energy which would be liberated during the slow stage.

To verify this assumption, a series of tests have been conducted where the steam flow was introduced into the reactor at different steady state temperatures at reaction zone, starting at 400 °C and higher. The steam flow into the reactor was turned off immediately after the completion of the fast stage. The typical hydrogen flow and its concentration in a sample case are presented in Fig. 3c, d.

4.2. Conversion of zinc as a function of temperature in reaction zone when the steam flow starts

This series of tests were carried out with the same amount of SOLZINC powder $M_0 \approx 9$–10 g ($C_{Zn}^0 = 0.847$) at near atmospheric pressure, constant carrier gas flow rate of $F_{N_2} = 100$–$110\,cm^3$/min and constant water flow $F_{H_2O} = 0.55$ g/ min (steam partial pressure without reaction $P_{H_2O}^0 \approx 0.93$ (bar abs)). Tests parameters and their main characteristics are listed in Table 3 including test results shown in Fig. 4 (corresponding to the first row in Table 3). For comparison, test results are presented for commercial Zn powder (by Sigma-Aldrich) with $C_{Zn}^0 = 0.98$ (last row in Table 3). Concentration of Zn in material left after the test, C_{Zn}(%), was measured with absolute accuracy of ±1% for four samples using Ultra III Rigaku X-ray powder diffractometer.

It should be noted that despite the fact that in most tests (except for test No. 1 Table 3, shown also in Fig. 4) the fast reaction starts together with the beginning of feeding the steam, and the steam flow was switched out when the fast stage was

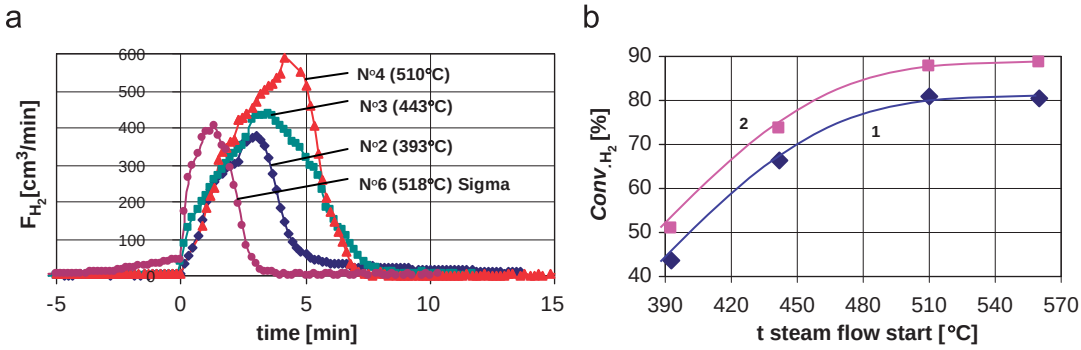

Fig. 5. Improving of reactivity in fast stage with increasing of temperature in reaction zone when the steam flow starts (a: hydrogen peaks; in parenthesis: temperature, when the steam flow started; b: SOLZINC conversion calculated for tests Nos. 2–5 as the ratio of hydrogen yield under peak (1) in fast stage and the total hydrogen yield during the test (2) to the theoretical amount of hydrogen).

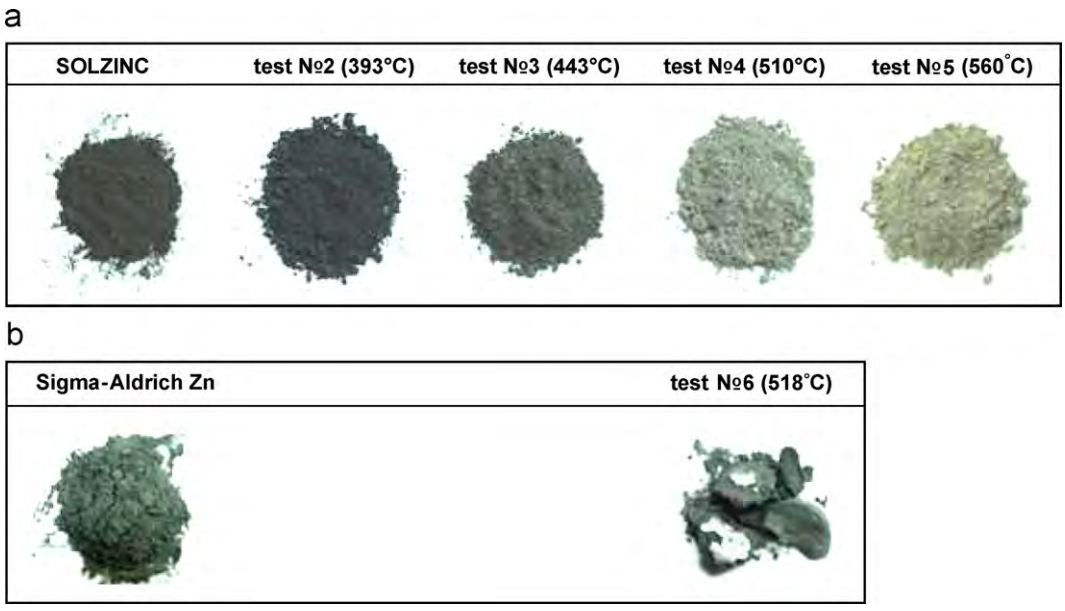

Fig. 6. Tested powders before and after tests: (a) SOLZINC, (b) commercial zinc (in parenthesis—temperature, when the steam flow started).

completed (except for test Nos. 1 and 6, where the reactions were continued after this stage during 100 and 45 min, respectively), the total conversion was about 7–8% higher than the conversion during the fast stage because hydrogen yield of 0.2 cm^3/min per gram of the initial powder is measured by the hydrogen analyzer when reaching a temperature of 300 °C in the reaction zone already before the steam flow started. The reason could be humidity in the reactor volume in spite of preheating for more than 1 h at $t = 100$–250 °C and flashing with dry nitrogen. On the other hand, the reaction continues during some minutes after steam had been switched off because of residual amount of water vapors.

A few important conclusions can be drawn from the data presented in Table 3:

1. Oxidation during the initial slow stage suppresses the developing of the fast stage (compare data for test Nos. 1 and 2, columns 10, 11) apparently due to the accumulation of additional 10–15% ZnO and the waste of the exothermic heat that potentially could be used later in the fast stage.
2. Reactivity of the SOLZINC, although containing larger amount of oxide a priori, is more than 3 times higher than the reactivity of commercial zinc powder (Sigma-Aldrich) at the same conditions (compare data for test Nos. 4 and 6, columns 10, 11 and Fig. 5a). When temperature of 450 °C is reached in reaction zone before the steam flow starts, relatively intensive vaporization of the commercial zinc begins (see curve No. 6 in Fig. 5a). Furthermore, it was possible to observe conglomerates and melted zinc fragments in the sample holder after the test. This was not observed in case of the SOLZINC (see Fig. 6) because this powder is more dispersed and contains higher initial amount of oxide.
3. Rising temperature of the reactor from 400 to 520 °C, before the steam flow starts, improves the conversion of SOLZINC twice but further increase of the temperature has, practically,

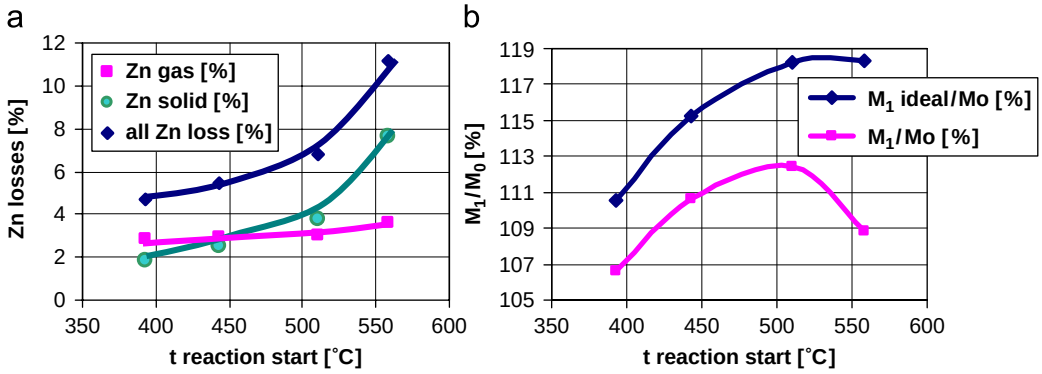

Fig. 7. Zinc losses (a) and relative mass of powder left after test (b) versus starting temperatures of the reaction.

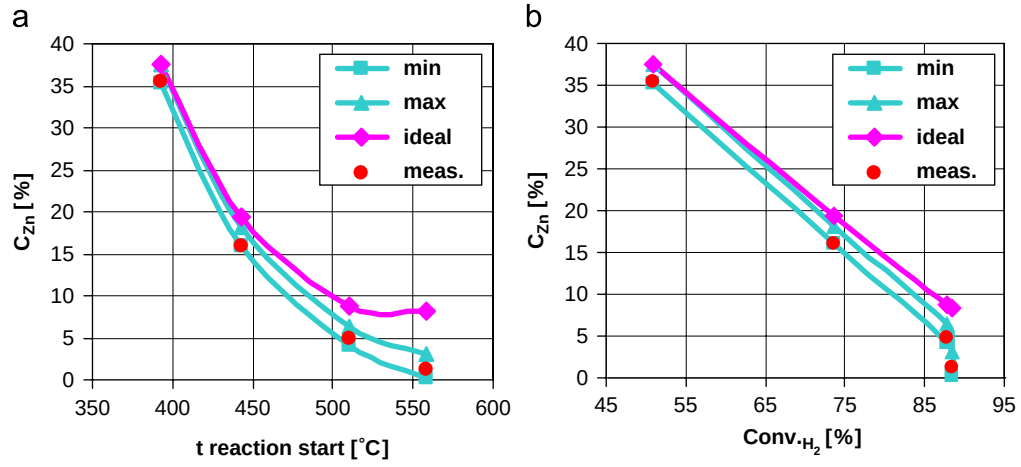

Fig. 8. Ideal Zn concentration C_{Zn}^{ideal} and real concentration interval $C_{Zn}^{min} < C_{Zn} < C_{Zn}^{max}$ (a) versus temperature of reaction start and (b) versus zinc conversion.

no effect on the conversion (see Table 3, columns 11, 12 and Fig. 5b) possibly because of the enlarging rate of non-reacted Zn losses (see Table 3, column 4 and in Section 4.3).

4.3. Estimation of the zinc losses and zinc concentration

Zinc solid, gas and total losses were estimated according to Eqs. (15), (18) and (14) with relative accuracy of 0.1%, 20–30% and 6–8%, respectively, for test Nos. 2–5 (Table 3) as a function of $t_{steam\ flow\ start}$ that corresponds in these cases to the reactor temperature when the fast reaction starts. The results are presented in Fig. 7a. It is possible to see that the rate of total losses L_{Zn} rises significantly above 500 °C because of the l_{Zn}^{solid}, which can be doubled (from 4% to 8%) at preheating temperature in the range of 510–560 °C, whereas the total gas losses remain almost at the same level with slight increase from 3% to 3.6% apparently due to faster rate of oxidation which decreases the rate of evaporation. The fact that the total zinc losses is increasing in parallel with ascending temperatures is evident also from the data in Fig. 7b, where it can be seen that ideal mass M_1^{ideal} estimated from Eq. (10) is always higher than the real mass of the powder left after the test, M_1, because of the zinc losses (the distinction between real and ideal mass is substantially increased at temperatures higher than 500 °C). Estimation of the zinc vapor losses, which can react with steam outside the sample holder or remain unreacted, can be made separately from Eqs. (16), (17). This assessment could have a significant error because of the poor accuracy of low concentration measurement of Zn and low absolute values of the losses. Nevertheless, these equations can be useful when estimating the possible Zn concentration range from Eqs. (19), (20) allowing the cross checking of the available data based on two independent measurements (concentration and conversion).

The ideal zinc concentration, C_{Zn}^{ideal}, and real concentration limits, C_{Zn}^{min} and C_{Zn}^{max}, in the remaining material versus the starting temperature of the reaction and versus zinc conversion calculated from Eqs. (11), (19) and (20) compared to the measurement zinc concentration C_{Zn} in residue powder are presented in Fig. 8. It can be seen that real concentration is always less than the ideal by 3–7% and this difference increases as the initial temperature and conversion are increasing because of the rising zinc losses at higher temperatures.

4.4. The structure of the powders before and after tests

To understand the difference in behavior between SOLZINC and commercial zinc, TEM analyses of the zinc powders before tests were done. Comparing their structures can explain the

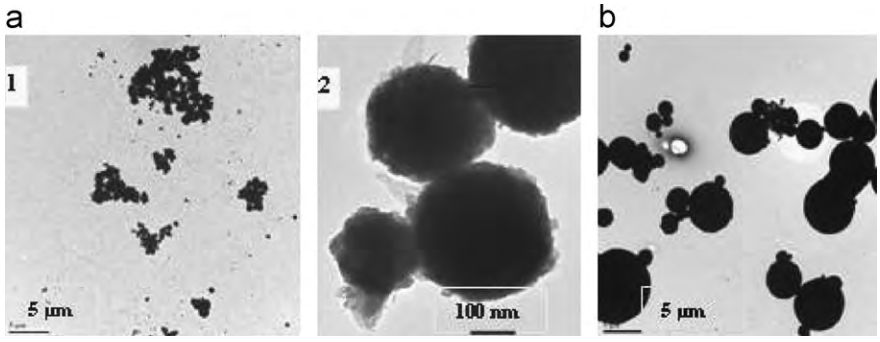

Fig. 9. Comparison of SOLZINC (a) and sigma zinc (b) structures.

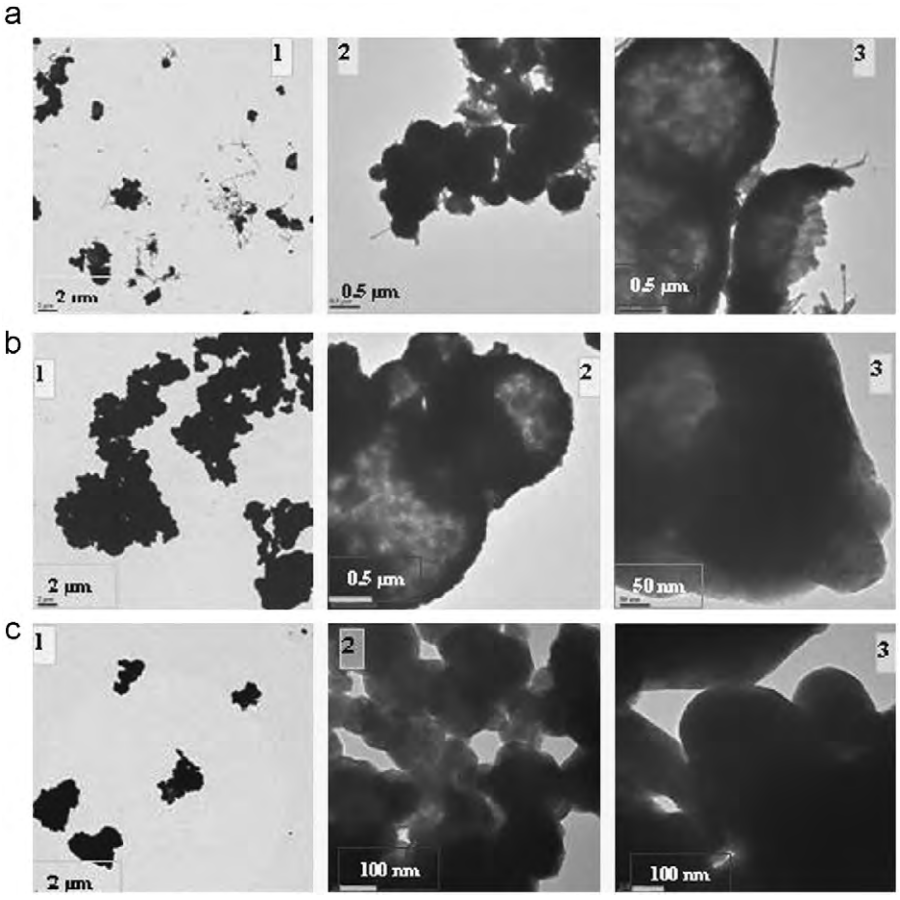

Fig. 10. Structures of hydrolyzed powder at (a) 50%, (b) 75% and (c) 90% conversion.

superior SOLZINC reactivity: it consists of 2–7 μm conglomerates (Fig. 9a-1) formed of very small spheres of 200–500 nm (Fig. 9a-2), whereas the commercial zinc particles are also spherical, but having significantly larger diameters that can reach 10 μm (Fig. 9b).

TEM analyses of SOLZINC powder after the hydrolysis tests show (see Fig. 10) that the spherical structure of the conglomerates partially remains up to 75% conversion. TEM pictures indicate that unlike current view about zinc oxide film formation the oxide crystallites can be formed not on the surface but inside the zinc particles causing them to burst out. Obviously, molecules of water penetrates inside the spheres (initial crystals of zinc oxide visible in Fig. 9a-2 can promote this), and the reaction is developed in the hottest space inside the spheres (see Fig. 10a-3 and b-2) which is broken up by ZnO crystallites (see Fig. 10a-3) and not on the particle surface which is cooled by the steam flow. This demonstrates once more that thermo-physical processes and heat transfer mechanism play an essential role in the hydrolysis process of the metal powder.

5. Conclusions

1. Experimental setup was built for studying the hydrolysis of metals for the production of hydrogen under controlled process parameters, such as temperature, pressure, steam and carrier gas flow rate and metal/steam ratio.
2. Results of batch experiments using 10 g solar produced zinc powder (from SOLZINC project) with water flow of 0.55 g/min and carrier gas flow 100 cc/min lead to the following conclusions:
   2.1. Specific structure of SOLZINC powder explains its fast and high conversion to ZnO powder without intermediate melting or evaporation of zinc.
   2.2. Zinc hydrolysis proceeds in two stages:
   2.2.1. *Fast stage*:
   - Spontaneous developing at $t \geqslant 400\,^{\circ}C$.
   - Strong increase of the temperature occurs in the reaction zone.
   - Hydrogen yield is very sensitive to the temperature in the reaction zone when the steam flow starts. It varies from 24% to 81% of the theoretical amount corresponding to temperature range of 185 to 560 °C, respectively.
   - Hydrogen yield decreases if partial oxidation of the zinc powder happens before the fast stage has developed.
   - Relatively high conversion values were achieved when the steam flow starts at reactor temperature of $t \approx 510\,^{\circ}C$, but further increase in temperature is accompanied by zinc losses of up to 11% because of zinc evaporation and its interaction with sample holder's material and does not result in higher conversion.
   - Reactivity of SOLZINC powder is significantly higher than the reactivity of a commercial zinc powder (by Sigma-Aldrich) at the same experimental conditions although it contains more zinc oxide before the hydrolysis took place, because of differences in their morphology.

   2.2.2. *Slow stage*:
   - Starting at $t > 300\,^{\circ}C$, and resuming after the fast stage terminates.
   - No second 'fast' reaction is observed up to 600 °C.
   - Its duration can be hours with gradual decreasing of the hydrogen output.
   - Hydrogen production rate is decreased after the 'fast' peak at similar operating conditions as before the peak due to the amount of zinc oxide in the sample holder.
   - Strong dependence of reactivity on temperature.
3. Further investigations are planned to understand better the process and optimize it in order to reach higher conversion and simultaneously decrease the zinc losses.

Acknowledgments

The authors would like to express their gratitude to Adi Arnon for his invaluable assistance in preparing and carrying out the experiments, to Ronit Popovitz-Biro for performing the TEM analyses of powders and to Yishay Feldman for measuring the zinc concentration.

References

[1] Bilgen E, Bilgen C. Solar hydrogen production using two-step thermochemical cycles. Int J Hydrogen Energy 1982;7:637–44.
[2] Steinfeld A. Solar thermochemical production of hydrogen—a review. Sol Energy 2005;78:603–15.
[3] Steinfeld A. Solar hydrogen production via two-step water splitting thermo chemical cycle based on Zn/ZnO redox reaction. Int J Hydrogen Energy 2002;27:611–9.
[4] Epstein M, Wieckert C, Olalde G, Santen S, et al. Towards an industrial solar carbothermic production of zinc. In: Proceedings of the 13th international symposium on solar power and chemical energy system, Seville, Spain, June 20–23, 2006, paper FB2-S6 (CD-publication), ISBN: 84-7834-519-1.
[5] Schunk L, Muller R, Meier A, Steinfield A. Solar thermal dissociation of zinc oxide in a semi-transient direct heating rotary reactor. In: International symposium on solar power and chemical energy system, Seville, Spain, June 20–23, 2006, paper FB2-S9 (CD-publication), ISBN: 84-7834-519-1.
[6] Weidenkaff A, Reller AW, Wokaun A, Steinfeld A. Thermogravimetric analysis of the ZnO/Zn water splitting cycle. Thermochim Acta 2000;359:69–75.
[7] Berman A, Epstein M. The kinetics of hydrogen production by oxidation of liquid zinc with water vapor. Int J Hydrogen Energy 2000;25:957–67.
[8] Ernst FO, Tricoly A, Steinfeld A, Pratsinis SE. Co-synthesis of H_2 and ZnO by in-situ Zn aerosol formation and hydrolysis. AIChE J 2006;52:3297–303.
[9] Vishnevetsky I, Epstein M, Abu-Hamed Tareq T, Karni J. Boron hydrolysis at moderate temperature. In: Proceedings of the 13th international symposium on solar power and chemical energy system, Seville, Spain, June 20–23, 2006, paper FB2-S13 (CD-publication), ISBN: 84-7834-519-1.